

## Stress-Strain Behavior of the Workings during the Rich Iron Ores Development under the Confined Aquifers

Vladimir Leonidovich Trushko, Anatoliy Grigoryevich Protosenya and Olga Vladimirovna Trushko

*Saint-Petersburg Mining University, Russia, 199106, Saint-Petersburg, 21-st Line V.O., 2*

### Abstract

The geological, hydrogeological and geotechnical conditions of the Yakovlevsky rich iron ores deposit development under the confined aquifers are analyzed. The deposit is unique in the ore stock and complexity of the mining and geological conditions, the ground waters head is 560 m. The deposit development is performed by the slicing system with the consolidating stowing in the downward direction without drainage. The field studies results concerning the stopes stability under the safety overlap are considered. It has been established that the loss in the workings stability in the rich friable ores is caused by their transit to the limit state and the shear zones formation in the working walls along the glide lines. The geomechanical forecast models of the solid ore stress-strain behavior around the stopes under the safety overlap were created. On the basis of the numerical studies, the shapes and dimensions of the limit state zones, as well as the concentration factors of the vertical intensities and the horizontal displacements of the rock ore were determined. For the workings stability improvement, it is suggested to change their cross-sectional shape from rectangular to trapezoidal profile. The trapezoidal profile stopes stability assessment was performed.

**Keywords:** iron ore deposit, ground waters head, stress, working, limit state, stability.

### INTRODUCTION

The Yakovlevsky iron ore deposit of the Kursk Magnetic Anomaly is unique by the ore stock of 9.6 billion tons and the ores quality with the iron content up to 69% among the discovered and the operated iron ore deposits at the present time.

From the structural point of view, the deposit is a syncline fold. The Yakovlevsky banded iron formation stripe borders with the western flank of the syncline fold mentioned above. The total length of the syncline exceeds 70 km, the syncline width within the proved area by the banded iron formation crops varies from 1.2 km to 1.6 km [1].

According to the data obtained during the geological exploration at the Yakovlevsky deposit area, the basement rocks, with which the rich iron ores are associated, occur under the sedimentation mass sheet at the depth of 470-550 m. The Lower Carboniferous limestone is the direct roof of the ores with thickness varying from 10 m to 50 m. The average trend of the basic deposit structure is north-western – 320°.

Generally, the rocks north-eastern dip angle within the slope mine varies from 60° to 70° [2].

The vertical thickness of the ore deposit lies within the wide range and varies from 20 m to 50 m near the footwall, from 100 m to 200 m in the middle section and goes up to 350-400 m near the side wall. The deposits width varies from 200 m to 600 m [3-4].

At the Yakovlevsky deposit as well as at the other KMA deposits the two genetic types of the rich iron ores can be distinguished: the parent or eluvial (residual) ores, that is, the laterization products of the banded iron formations of different types, and the redeposited (aqueous) ores, that is, the products of the parent ores washing-out and redeposition. The redeposited ores are tributary, their content is approximately 3-5% of the total ore stock.

The following ores types are distinguished by mineral composition within the primary mining area:

- iron-micaceous-martite and martite-iron-micaceous friable ores;
- iron-micaceous-martite chloritized and carbonatized ores;
- hydrohematite-martite and goethite-hydrohematite semifriable ores;
- carbonatized ores.

Each ore type mentioned above corresponds to the definite type of the banded iron formations, which predetermines their spatial isolation.

Generally the parent ores are presented at the deposit by the friable fine-pored varieties of the iron-micaceous and iron-micaceous-martite structure, the present ores content is approximately 59.5% of the total stock. The ores are of the faint bluish tinge; therefore, they were named the “blue ores”. By the physical properties, the ores are friable powdery pored with poor structural bond.

The hydrohematite-martite ores, that is, the “blue ores”, are rather widely spread at the deposit; their content is 25.2% of the total stock. The ores have the layer-by-layer maculose color from dark red to brownish. The ores are usually weak, poorly consolidated with thin-slabby parting.

The iron content depends on the ores mineral composition. The average iron content on the primary mining area is 62%.

The moisture content in the natural ores varies from 5.3% in solid ores to 17.2% in the friable ores; the average moisture content is 9.8%.

The Yakovlevsky deposit is characterized by the high degree of invasion; the total width of the invasion zone exceeds 700

meters. The following parameters can be referred to the basic hydrogeological features of the deposit: the great depth of the rich iron ores; complex conditions of the ore deposit invasion; hydraulic connection of the crystalline-ore aquifer with overlying lower carboniferous horizon; the sedimentary rocks of seven aquifers in the strata characterized by the large hydraulic heads, and the wide variation range of the waters chemical composition [1-2].

The aquifers of the sedimentation rock top level are characterized by the pressureless mode and, consequently, have no impact on the ore deposit invasion. The aquifers of the Carbonic period are not divided by the persistent aquicludes and form the unified aquifer system with heads up to 480 m.

It was established during the hydrogeological research conduction that the Lower Carboniferous and the crystalline-ore horizons are the basic aquifers which have an impact on the water inflows in the underground workings during the Yakovlevsky mine development. Both horizons have the hydraulic connection [5].

The Lower Carboniferous aquifer which occurs above the ore body is connected with the fractured and karst limestones, less often – with sands and sandstones. The depth of the aquifer footwall occurrence is 500-550 m, the width is 20-80 m, and the productive head exceeded 350 m in 2010 year. The transmission constants vary from 0.01 meters per day to 12 meters per day depending on the rocks fracture intensity and cavernous porosity. In the deeper section of the coal formation, there is a limestones band with the width of 6.0-22.5 m, with underlying rich iron ores (RIO), which form the double-layer water-resistant strata.

The crystalline-ore aquifer borders with the rocks of the weathering crust fracture zone of Precambrian crystalline formations as well as the fault zones formations and is presented by the iron ores, banded iron formations and shales. The depth of the aquifer occurrence is 450-690 m. The aquifer is confined, the head above the roof is 450-560 meters in case of undisturbed conditions. The aquifer is drained within the slope mine. The conditions of the ground waters filtration in the inhomogeneous strata are complicated. They are defined by the rocks porosity and fracture intensity. The rich iron ores are characterized by the transmission constant which varies from 0.04 to 0.28 meters per day. The shales and quartz rocks transmission constant is less than 0.01 meters per day [3-4].

At the present time, the ore body draining is being performed from the rock workings horizon -425 m at the Yakovlevsky mine by means of horizontal and inclined blow-out wells. The large heads at the overlying aquifers are remained.

The ore body mining without the quaternary deposits draining is possible only in case of the waterproof properties retention of the Carbonic period rocks, by means of prevention of the water-conduction fractures formation.

The ground waters breakthrough from the Lower Carboniferous aquifer is the most dangerous factor, which can result in the irreversible effects and failures during the mine development and operation [6-7].

Within the framework of the hydrogeochemical and hydrodynamical monitoring at the Yakovlevsky mine, the draining wells and the water inflows in the underground workings of the -425 m and -370 m horizons, as well as the exterior observation wells were inspected during the period of 2006 to 2012 with the help of the Mining University members and the mine and geologic-surveying division. According to the undertaken studies' data, the change in the absolute elevation levels of the Lower Carboniferous aquifer ground waters indicates that there is a possible stimulation of the waters flow from the undrained Lower Carboniferous aquifer to the crystalline-ore horizon. In future, it can have an adverse effect on safety ore floor pillar stability and mining safety.

At the present time in Russia and in majority of countries, the large unwatered ore deposits with considerable amount of easily accessible stocks are nearly worked. Further development of the raw-materials base in many regions is related to the necessity of the deep-seated water-bearing deposits development, characterized by rather complicated hydrogeological conditions.

One of the most effective methods of the deposits development under the aquifers without the overburden draining is the reservation of the safety floor pillar which prevents the waters inflow in the rock workings [8-9]. During the deposits development with the high degree of invasion, the development systems with stowing are used in the majority of cases. The use of the consolidating stowing during the processing procedures of the ore production permits to decrease the losses and delution of the rock ore, minimize the negative impact of the mining operations on the water-resistant strata, work out the ores stock in protective pillars and protect the earth surface against caving by means of the mining operations safety ensuring [10].

Let us consider the ore deposits, the development of which is performed under the undrained flooded strata under the complex mining geological conditions.

The mining plant named after Gubkin develops the Korobkovsky deposit of the KMA. The banded iron formations are overlapped by the thick mass of the flooded sandy and clay rocks liable to transition to the running state. Originally, the rich iron ores work out was the purpose of the mine development, but due to the numerous water and drift sand breakthroughs in the rock workings the rich ores could not be worked out, and it was decided to use the driven openings for the banded iron formations production. The ore production by the pillar-and-breast system is performed within one extraction level with the height of 60 m under the protection of the safety ore floor pillar with the width of 70-100 m, supported by the interchamber pillars system. The ore losses there reach 57-60%, which along with the "floor pillar-chambers-pillars" structure safety margin induces considerable losses of the field ore. The water inflow in the ground rock workings reaches the value of 300 m<sup>3</sup>/hour [11].

The Zaporozhian mining plant develops the Yuzhno-Belozersky rich iron ores deposit with Fe content up to 62%. The reservoir thickness varies from 80 m in the northern side to 230 m in the southern side. The dip is heavy at the angle of 65-70° to the east. The following factors complicate the

deposit development: the mining depth up to 600 m, the presence of seven aquifers in the sandy and clay deposits' overburden characterized by the large hydraulic heads up to 200 m. Due to the hydrogeological conditions complexity, the pillar-and-breast system with sublevel ore breaking with further stowing by consolidating mixtures was used. The ore production is performed under the protection of the safety ore floor pillar with the width of 60 m. The level height is 100 m, the chamber width is 30 m.

The Yakovlevsky rich iron ores deposit is developed under the protection of the safety ore floor pillar with the width of 65 m and artificial overlap presented by the network of parallel horizontal workings filled by solid consolidating mixture [5].

The development system with layers mining in descending order, continuous ore breaking and solid consolidating stowing is one of the most commonly used systems under the complex mining conditions. Due to the ore low strength, the mechanical ore separation from the rock mass by the boom miners was used. The safety floor pillar formation and the underlying layers work out are performed by the stopes with the width of 4.9 m. The layers height chosen on the base of the boom miner parameters is 4 m [13-14].

#### METHODOLOGY: Investigation and Calculation of the Stress-Strain Behavior

The rock workings survey was performed with the purpose of determination of behavior of the timber actual state and the workings stability during the broken working expansion.

The rock workings survey form was developed. It comprised the following:

- Visual inspection of the timber and the ore cropping state;
- Measurement of basic dimensions of the timber of single workings and junctions;
- Measurement of the overbreak values of the supporting area in the walls and on the roof;
- Determination of the rocks sloughing zones in the working walls at the junctions;
- Assessment of the timber state in single workings and junctions, including the timber elements deformation and damage character;
- Measurement of the workings dimensions at the rock inrush areas;
- Fixation of the discovered defects of the timber elements.

Numerical simulation on the basis of the finite elements method (FEM) was used for investigation of the stress-strain behavior of the rock mass around the workings under the safety overlap. Despite the idealization of the actual conditions, the use of FEM permits to bring the calculation model near to the real object and also provides an opportunity to study the object within the wide range of conditions by means of the change of the medium properties and geometrical parameters of the model. The method is based on numerical calculation of the partial differential equations system.

Numerical simulation of the workings driving and flushing is performed in the plane deformation statement. The real rock mass was considered as the solid medium and it was changed by the significant finite domain with the width of 1300 m and the height of 200 m (Figure 1). The model dimensions were selected in such a way as to eliminate the boundary conditions influence on the stresses and strains distributions around the workings.

The boundary conditions are as follows: the displacements along the domain lateral edges were prohibited in X-direction, along the bottom edge – in Y-direction, the top edge of the domain remained freely deformable. The safety overlap is located at the depth of 65 m from the model top edge, which corresponds to the rock ore dimensions above the top layer (safety ore pillar).

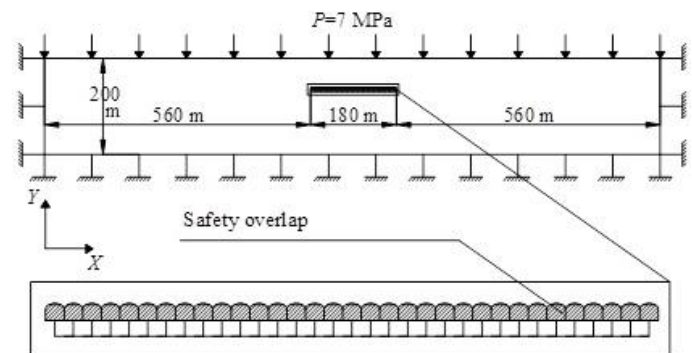


Figure 1. Principle diagram used in the finite-element model

The natural strain-stress behavior of the rock mass was prescribed by vertical intensities  $\sigma_v = 7$  MPa, exerted on the top edge of the finite-element model. The vertical intensities value was taken in accordance with the previous calculations of the inhomogeneous rock mass stress-strain state caused by draining of the primary work out area at the boundary "Carboniferous limestone-ore body" [15].

Discretization of the model calculation domain was implemented in such a manner that the minimum dimension of the finite element was 0.3 meters on the workings contour, and the maximum dimension with distance from the workings line was 5 meters. Thereby, the finite elements mesh refinement was performed in the neighborhood of the workings. The flat four-node finite elements of the first order were used as the finite elements type.

The Yakovlevsky deposit ores have contained plasticity.

The processes of elasto-plastic deformation of the rocks occur around the workings with nonlinear deformations zones formation [16-17]. The Mohr-Coulomb elasto-plastic model of the rocks deformation was taken as a model for the stress-strain behavior investigation.

The enclosing rock ore is presented by the nonlinearly-deformable isotropic medium with stress-strain properties of the iron-micaceous-martite ore (Table 1).

**Table 1.** Stress-strain properties of the rich iron ores (RIO), determined on the undisturbed and disturbed structure samples under the conditions of natural flooding, complete draining and secondary water treatment

No.	Ore characteristics and sampling area	Specific weight, $\text{kN/m}^3 \times 10^{-1}$	Moisture content, %	Porosity, %	Degree of water saturation, G	Shear resistance parameters		Compression strength $R_{\text{comp}}$ , MPa	Structural strain modulus $E_s$ , MPa
						Coupling, MPa	Angle of		
Ore of undisturbed structure									
1	Undrained ores (haulage ort hor. -425 m)	<u>3.26-3.45</u> 3.38	<u>12.3-13.6</u> 13.2	<u>42.2-43.3</u> 42.7	<u>0.84-0.98</u> 0.95	<u>0.025-0.5</u> 0.36	8-9	<u>0.058-1.15</u> 0.83	<u>31.0-105.0</u> 63
2	Drained ores (experimental roadway. hor. -425 m, decompression zone)	<u>2.36-2.82</u> 2.6	<u>4.1-10.8</u> 6.9	<u>49.8-56.8</u> 53.7	<u>0.20-0.53</u> 0.31	<u>0.15-0.80</u> 0.36	23	<u>0.45-2.42</u> 1.087	<u>18.0-27.0</u> 21.0
3	Secondary watered ores	<u>2.68-3.07</u> 2.84	<u>12.6</u> 12.6	<u>47.9-54.3</u> 51.4	<u>0.58-0.68</u> 0.62	< 0.08	< 8	0.184	-
Ore of disturbed structure									
4	Water-saturated iron-micaceous-martite and martite ores	<u>3.14-3.30</u> 3.21	<u>12.0-15.0</u> 13.5	<u>43.2-45.5</u> 44.1	<u>0.95</u> 0.95	<u>0.28-0.38</u> 0.33	<u>6-13</u> 8	<u>0.62-0.95</u> 0.759	-
	The same but dry ores	<u>2.88-3.45</u> 3.19	<u>4-10</u> 6.1	<u>42.8-46.7</u> 44.3	<u>0.22-0.50</u> 0.33	<u>0.1-0.38</u> 0.21	<u>23-28</u> 24	<u>0.302-1.26</u> 0.647	-
5	Water-saturated hydrohematite ores (paint)	<u>2.74-2.85</u> 2.80	<u>15.0-16.5</u> 16	<u>44.2-48.4</u> 45.4	0.98	<u>0.45-0.68</u> 0.53	<u>7-12</u> 0.53	<u>1.02-1.679</u> 1.24	-

The model comprises driving and flushing of 37 workings at the top bearing layer of the safety overlap of Block No. 4 and driving of 36 workings under the safety overlap. At the present time, the mining operation scheme with leaving the dividing pillar with the width of two working spans between the first stage stopes is taken as the basic version, as far as it is preferred in the context of reservation of the safety strata under the aquifer system.

**The problem is solved in three stages.**

**The first stage** is calculated by means of the geostatic solver, which permits to exclude the so-called “historical” displacements. The rock ore with no weaknesses in the form of workings was considered. The present stage was necessary for field creation of the rock natural stress state. For the present purpose, the gravitational forces with gravitational acceleration value equal to  $9.81 \text{ m/s}^2$  were applied to the rock ore and the vertical load  $P = 7 \text{ MPa}$  was exerted on the model top edge. In this case, due to the mathematical statement peculiarities of the program solver applied at the present stage, any rock ore displacements under the load were prohibited. As a consequence, the stress field was formed in the rock ore which prevented the displacements under the gravitational forces; in other words, the static equilibrium state occurred. The obtained stress field can be considered as the natural stress state field of the rock ore.

**The second stage.** The safety overlap formation.

At the present stage, the sequential driving of the safety overlap workings was simulated and the stress and strain fields were investigated in the zone, where the second layer workings will be driven in future: simulation of the first stage safety overlap workings driving at the distance of two working spans; flushing of the first stage workings; driving of the second stage workings adjacent to the filling mass of the first stage working; flushing of the second stage workings; driving of the stopes along the pillar between the concrete bands; the third stage workings flushing.

The convergence of the rock ore vertical displacements and the field data was investigated.

**The third stage.** The workings driving under the safety overlap.

The workings under the safety overlap are driven in a similar sequence as during the safety overlap formation.

**RESULTS**

**1. Stress-strain properties of the ores, the enclosing rocks and the filling mass**

The rocks and the compact ores properties were determined on the core samples obtained by the exploration wells drilling. Collection of the ores core samples with poor structural bonds turned to be impossible; therefore, the friable ores properties were determined on the samples, obtained by compaction under the loads corresponding to the overburden pressure [4].

The experimental data, obtained on the compacted samples, gives the approximate data concerning the rich iron ores properties in the natural state.

During driving of the workings of hor. -425 m along the rock ore, the members of the mine geological survey and the mining University have collected the monoliths of different ore types, from which the samples with natural moisture content, drained and remoistened, were produced and tested in the Mining University laboratories. The samples were obtained from the rock ore cropping, subject to the explosion overpressure, bearing pressure during the workings driving

and the weathering agents impact. The obtained test results are presented in Table 2 [4].

During the further investigations of the friable ores properties under the mine conditions, the members of the Mining University have developed the technique of the friable iron-micaceous ore strength determination by drilling [15-16]. It was established during the natural tests conduction that the rock ore strength in the near-contour layer differs markedly from the similar index in case of location the depth. At the depth of 0.8-1.1 m from the rock cropping the ores strength is practically a sequence higher.

**Table 2.** Stress-strain properties of the ores and rocks between the -365 m and -425 m horizons

Ores and rocks title	Specific weight, $\text{kN/m}^3 \times 10^{-1}$	Porosity p, %	Breakdown point		Angle of internal friction $\rho$ , degrees	Specific coupling C, MPa	Strain modulus E, $\times 10^3$ MPa	Poisson ratio $\mu$
			Compression strength R, MPa	Tensile strength $\sigma_t$ , MPa				
1	2	3	4	5	6	7	8	9
<b>Martite ore</b>								
weak, friable	<u>3.02-3.54</u> 3.65	<u>17.4-23.6</u> 21.4	<u>0.7-2.7</u> 1.02	<u>0.2-0.5</u> 0.3	<u>20-35</u> 27	<u>0.3-0.7</u> 0.5	<u>1.16-2.4</u> 1.52	<u>0.24-0.3</u> 0.27
chloritized, middle-density	<u>3.10-3.60</u> 3.37	<u>12.1-19.6</u> 16.3	<u>2.4-9.3</u> 5.7	<u>0.6-2.5</u> 1.3	<u>32-37</u> 35	<u>0.8-1.7</u> 1.5	<u>1.56-3.02</u> 1.86	<u>0.22-0.27</u> 0.26
carbonatized, compact	<u>3.22-3.67</u> 3.41	<u>9.3-18.4</u> 14.6	<u>8.6-39.0</u> 20.1	<u>2.4-7.6</u> 4.9	<u>34-39</u> 37	<u>4.6-6.8</u> 5.3	<u>2.24-3.18</u> 2.67	<u>0.23-0.26</u> 0.24
<b>Iron-micaceous-martite ore</b>								
weak, friable	<u>3.17-3.63</u> 3.41	<u>17.2-24.3</u> 20.8	<u>0.5-2.8</u> 1.2	<u>0.2-0.4</u> 0.3	<u>20-36</u> 28	<u>0.1-0.6</u> 0.4	<u>1.34-2.23</u> 1.86	<u>0.22-0.30</u> 0.26
chloritized, middle-density	<u>3.31</u> 3.48	<u>14.7-21.7</u> 18.8	<u>1.9-7.6</u> 5.1	<u>0.7-1.9</u> 1.3	<u>32-38</u> 36	<u>0.9-2.7</u> 1.4	<u>1.54-2.47</u> 1.92	<u>0.21-0.29</u> 0.26
carbonatized, compact	<u>3.34-3.84</u> 3.58	<u>8.6-17.7</u> 12.4	<u>6.5-31.4</u> 16.7	<u>1.7-5.7</u> 4.0	<u>36-41</u> 38	<u>3.4-5.9</u> 4.3	<u>2.01-2.57</u> 2.23	<u>0.20-0.26</u> 0.24
<b>Hydrohematite-martite ore</b>								
clayline, weak, friable	<u>3.18-3.46</u> 3.28	<u>14.6-29.6</u> 25.8	<u>1.4-2.6</u> 2.1	<u>0.3-1.1</u> 0.6	<u>27-38</u> 34	<u>0.2-0.7</u> 0.6	<u>1.30-2.35</u> 1.74	<u>0.28-0.30</u> 0.29
clayline, chloritized, middle-density	<u>3.23-3.57</u> 3.34	<u>15.9-27.3</u> 19.3	<u>2.6-8.4</u> 6.9	<u>0.9-3.0</u> 1.9	<u>32-39</u> 35	<u>0.6-2.7</u> 1.8	<u>1.60-2.42</u> 1.92	<u>0.23-0.28</u> 0.25
clayline, carbonatized, compact	<u>3.20-3.84</u> 3.46	<u>10.8-21.3</u> 15.1	<u>7.3-43.6</u> 19.4	<u>2.7-6.7</u> 4.6	<u>34-40</u> 38	<u>2.5-7.6</u> 5.8	<u>1.60-2.74</u> 2.42	<u>0.21-0.28</u> 0.24

The analysis of the presented data shows that the properties of the ores of different mineral composition differ markedly. The values of the uniaxial compressive strength of the compact martite and hydrohematite-martite ores vary from 16.7 to 20.1 MPa, specific coupling values vary from 4.3 to 5.8 MPa, and the angles of internal friction vary from 35 to 38°.

The uniaxial compressive strength of the friable ores varies within the range of 1.02-2.1 MPa, specific coupling – 0.4-0.6 MPa, angles of internal friction – 27°-34°. The ores are characterized by high porosity, which reaches the value of 42% for friable ores.

Determination of the shear resistance parameters was performed in the single-plane shear devices at the normal pressures, which prevented the tearing strains development and the tension stresses formation, which leads to samples strength comprising and overestimation of the friction angles values.

## 2. The results of the field studies over the stability of the stopes driven under the safety overlap

During conduction of the field studies over the state of the mine workings under the Yakovlevsky mine safety overlap, the workings of the stopes No. 1, 4 and 6 were inspected. All the workings were driven by the combine method; the cross-sectional dimensions as per the design are as follows: the height is 4 m, the width is 4.9 m.

The mine workings, driven generally in the matrite-hydromartite ore with the hardness factor of  $f=2-4$ , where

$$f = \frac{\sigma_t}{10 \text{ MPa}}, \sigma_t \text{ is the ore tensile strength in uniaxial}$$

compression, MPa, were investigated in the stopes No. 1 and 6. During the workings inspection, the cleavages in the workings walls were revealed. The cleavages are systematic, and they more often occur at the contact with the friable ore band without structural bonds  $f < 1$  and geological faults of the rock mass. The split thickness is 0.3-0.5 m, the blocks are the ellipses extended by lamination, with the length up to 1.5-2 m and the height up to 2 m. The local developments of the water drip in the roof were detected, no impact of the water inflows on the mine workings stability was found. Generally, the workings driven under the safety overlap in the compact ores after the walls scalling maintain stability without the ore cappings supporting, the sections dimensions are close to the design dimensions during the whole period of the workings maintenance.

The fine-grained and fine-laminated mine workings, driven in the iron-micaceous-martite ores, with the hardness  $f \leq 1$ , with no structural bonds in some places, were inspected in the Block No. 4. The rock mass is unsteady. Along the whole length of the workings, the large ore cleavages from the walls are found, the cleavages depth in the roof reaches 0.8-1.3 m. The actual contour of the unsupported working is of the trapezoid form with the long base in the roof; its actual dimensions are inconsistent with the design dimensions. There is no core, the stable condition of the ore cappings is not provided. Usually, the workings are driven the next but three with dividing pillars of different width, the workings are stowed by the consolidating mixture, then the second, the third and the fourth stage workings are driven adjacent to the concrete filling.

The summary data with the results of the field studies over the state of 14 mine workings under the safety overlap are presented in Table 3.

On the basis of the field studies results, it was established that during the mine workings driving in the friable ores under the safety overlap the rock fragmentation is characterized by the shear surfaces formation in the working walls, the parameters of which depend heavily on the stress-strain properties of the ore. The workings lose stability, the safety operation conditions are not ensured.

In the Block No. 4, the cleavages from the workings walls, driven under the safety overlap, are found along the whole workings length. The average dimensions of the prills near the working roof reach 1.0-1.2 m, the shear surface slop angle is  $60^\circ$ . The volume of the prills on the definite intervals of the mine workings reaches  $15.5 \text{ m}^3$ .

The inspected mine workings of the blocks No. 1 and No. 6, driven in the compact ores, maintain stability without supporting after the walls scalling during the whole operation period until their flushing.

**Table 3.** Summary data of the field studies over the state of the mine workings under the safety overlap

Item No.	Working title	Core type	Characteristics of the enclosing rock mass. Driving conditions	Stability condition of the working	Buckling modes
1	2	3	4	5	6
1	Block No. 6, stope No. 8	No core	Hydrohematite compact ore, between the filled workings	The roof and the walls maintain stability	Water drip from the roof. Local sections of the filling mass with fractures in the walls
2	Block No. 6, stope No. 2	Mine woods from the ore cropping side, without lagging at 2-3 m interval	Iron-micaceous-martite, semifriable (0-38 m) and hydrohematite compact ore (70-250 m), adjacent to the filling mass	There are areas with cleavages from the ore cropping side at the section 0-38 m. Generally the roof and the walls maintain stability	Prills in the form of ellipse. There are several sections with the length of 1-2 m with the concrete cleavages from the walls
3	Block No. 6, stope No. 12	Mine woods from the ore cropping side, without lagging at 2-4 m interval.	Iron-micaceous-martite, semifriable (0-45 m) and hydrohematite compact ore (80-250 m), adjacent to the filling mass 6-1-11	There are the areas with intense cleavages from the ore cropping side at the section 0-45 m. The roof and the walls maintain stability	Water drip from the roof. Prills in the form of ellipse, with the depth up to 0.5 m

4	Block No. 6, stope No. 19	Mine woods, without lagging at 2-3 m interval	Iron-micaceous-martite, semifriable (0-58 m) and hydrohematite compact ore (165-222 m)	There are areas with intense cleavages from the ore cropping side at the section 0-58 m. The roof and the walls maintain stability	Prills in the form of ellipse, with depth up to 0.2-0.35 m
5	Block No. 6, stope No. 24	Mine woods from the ore cropping side, without lagging at 2-4 m interval.	Iron-micaceous-martite, semifriable (28-81 m) and martite-hydrohematite compact and semifriable ore, adjacent to the filling mass 6-1-23	The roof and the walls maintain stability	Local sections with the filling mass splits.
6	Block No. 6, stope No. 1	Mine woods from the ore cropping side, without lagging at 2-4 m interval.	Martite-hydrohematite, semifriable ore, adjacent to the filling mass 6-1-2	The roof and the walls maintain stability	Local sections with the filling mass splits. Water drip
7	Block No. 1, stope No. 1B	No core	Predominantly martite-hydrohematite, semifriable ore	There are cleavages in the walls at the friable ore sections. The roof and the walls maintain stability at the semifriable ore sections	Cleavages from the walls at the friable ore section, prills with thickness up to 0.5 m
8	Block No. 1, stope No. 3B	No core	Predominantly martite-hydrohematite, semifriable ore	There are cleavages in the walls at the friable ore sections. The roof and the walls maintain stability at the semifriable ore sections	Cleavages from the walls at the section of the friable ore and clayline hydrogoethite bands, prills with thickness up to 0.5 m
9	Block No. 1, stope No. 7B	No core	Predominantly martite-hydrohematite, semifriable ore	There are cleavages in the walls at the friable ore sections. The roof and the walls maintain stability at the semifriable ore sections	Cleavages from the walls at the section of the friable ore and clayline hydrogoethite bands, prills with thickness up to 0.5 m
10	Block No. 4, stope No. 6	No core	Iron-micaceous-martite friable ore	Unstable state, there are cleavages from the walls along the whole working length	Detached prills in the form of prism with thickness near the roof up to 1.2 m
11	Block No. 4, stope No. 9	No core	Iron-micaceous-martite friable ore	Unstable state, there are cleavages from the walls along the whole working length	Detached prills in the form of prism with thickness near the roof up to 1.1 m
12	Block No. 4, stope No. 12	No core	Iron-micaceous-martite friable ore	Unstable state, there are cleavages from the walls along the whole working length	Detached prills in the form of prism with thickness near the roof up to 1.1 m
13	Block No. 4, stope No. 11	No core	Iron-micaceous-martite friable ore	Unstable state, there are cleavages from the walls along the whole working length	Detached prills in the form of prism with thickness near the roof up to 1.1 m
14	Block No. 4, stope No. 14	No core	Iron-micaceous-martite friable ore	Unstable state, there are cleavages from the walls along the whole working length	Detached prills in the form of prism with thickness near the roof up to 1.0 m

### 3. Stress-strain behavior of the rock mass around the single rectangular profile workings under the safety overlap with consideration of contact interaction of the rock ore and the filling mass

The contact which assumes the possibility of the rock ore and safety overlap movement was considered for analysis of the rock and the filling mass contact interaction impact on the strain and stress fields distribution around the working under the safety overlap.

The configurations and dimensions of the limit state zone of the friable ore mass, enclosing a single working in case of the safety overlap contact with the rock ore, are presented in Figure 2.

The limit state zone configuration, presented in Figure 2, was obtained in case of contact with frictional drag coefficient of  $F = 0.35-0.45$ . It is in good agreement with the field studies data. The shear surface is formed at the contact of the rock ore and the safety overlap at the distance of 1.2 m from the working contour and is directed at an angle of  $68^\circ$ .

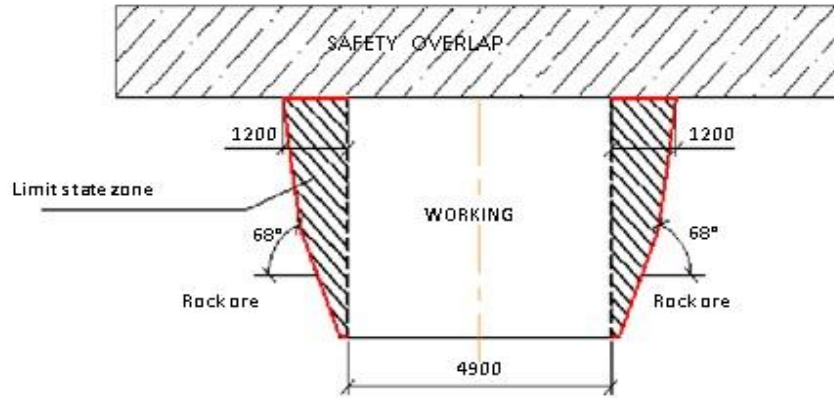


**Figure 2.** The limit state zone formation in the walls of the working under the safety overlap

The regularities of the vertical stresses concentration factor  $k$  change were obtained on the basis of the calculations results for qualitative evaluation of the rock ore stress-strain behavior and determination of the influence zone of the rock ore driven under the safety overlap.

The horizontal displacements in case of the contact with frictional drag coefficient ( $F = 0.35-0.45$ ) are spread deep into the rock ore at the distance of 3.0 m, the working contour near the roof is displaced by 25 mm, with the increase of the distance to the working roof the displacements are decreased (Figure 3).

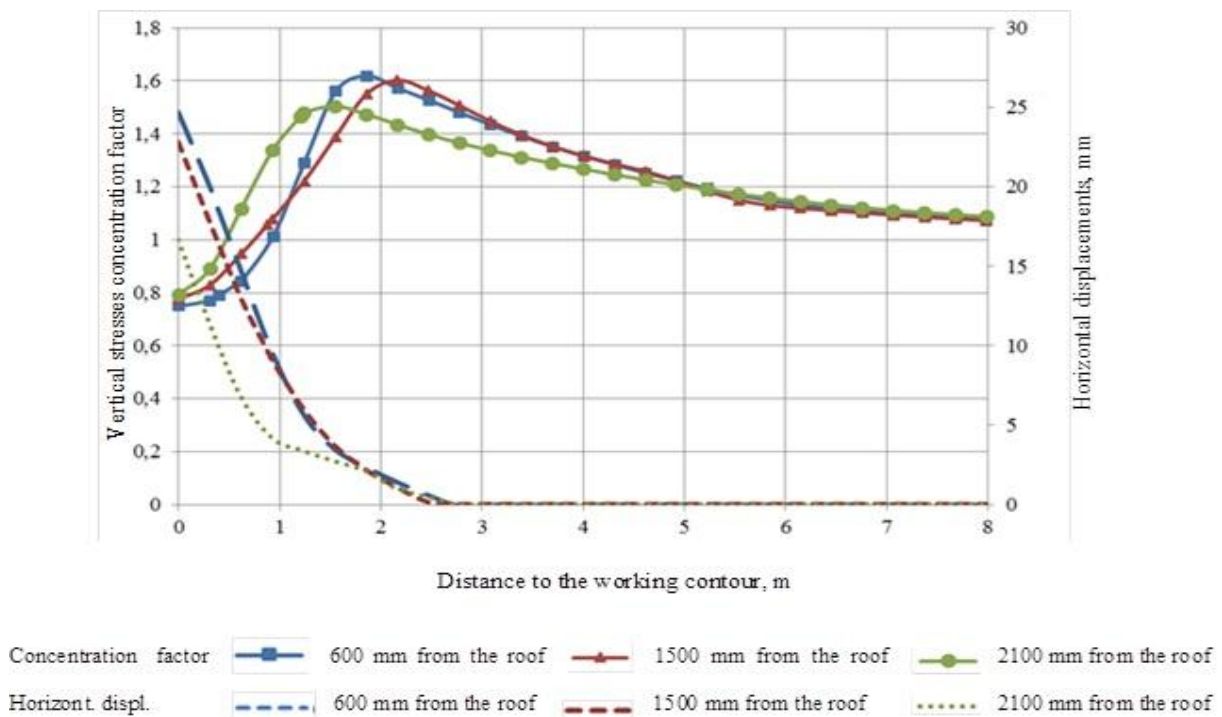


**Figure 3.** Distribution of the vertical stresses concentration factor and horizontal displacements in the wall of the working under the safety overlap

The intensive growth of the horizontal displacements is observed at the distance of 1.2 m to the working contour, which corresponds to the limit state domain boundary.

Maximum concentrations of the vertical stresses  $k = 1.62$  are observed at the distance of 2.0 m to the working contour. In the limit state zone, at the distance up to 1.0 m to the working contour,  $k = 0.7-1.0$ . The working influence zone is 8 m.

In the rock mass presented by the compact rich iron ore, the horizontal displacements are spread deep into the rock ore at the distance up to 1.5 m. In this case, the working contour near the roof is displaced by 2 mm, and the maximum displacements equal to 4 mm are observed at the height of 2.1 m from the roof.

The maximum concentrations of the vertical stresses  $k = 1.66$  are observed directly on the working contour at the height of 2.1 m from the roof. It should be also mentioned that at the

distance to the contour more than 3.0 m there is practically complete coincidence of the stresses concentrations factors change curves. The working influence zone is approximately 7-8 m.

The buckling mechanism of the ore croppings of the working walls under the safety overlap, determined during the numerical simulation, is supported by the field studies data.

#### 4. Numerical simulation of the rock ore strain-stress behavior during the trapezoidal mine workings driving under the safety overlap

For assessment of the rock ore stress-strain behavior and determination of the influence zone of the stope driven under the safety overlap, the regulations of the vertical stresses concentration factor and the horizontal displacements change in the working wall in case of displacement from the working contour deep into the rock ore were obtained (Figure 4).

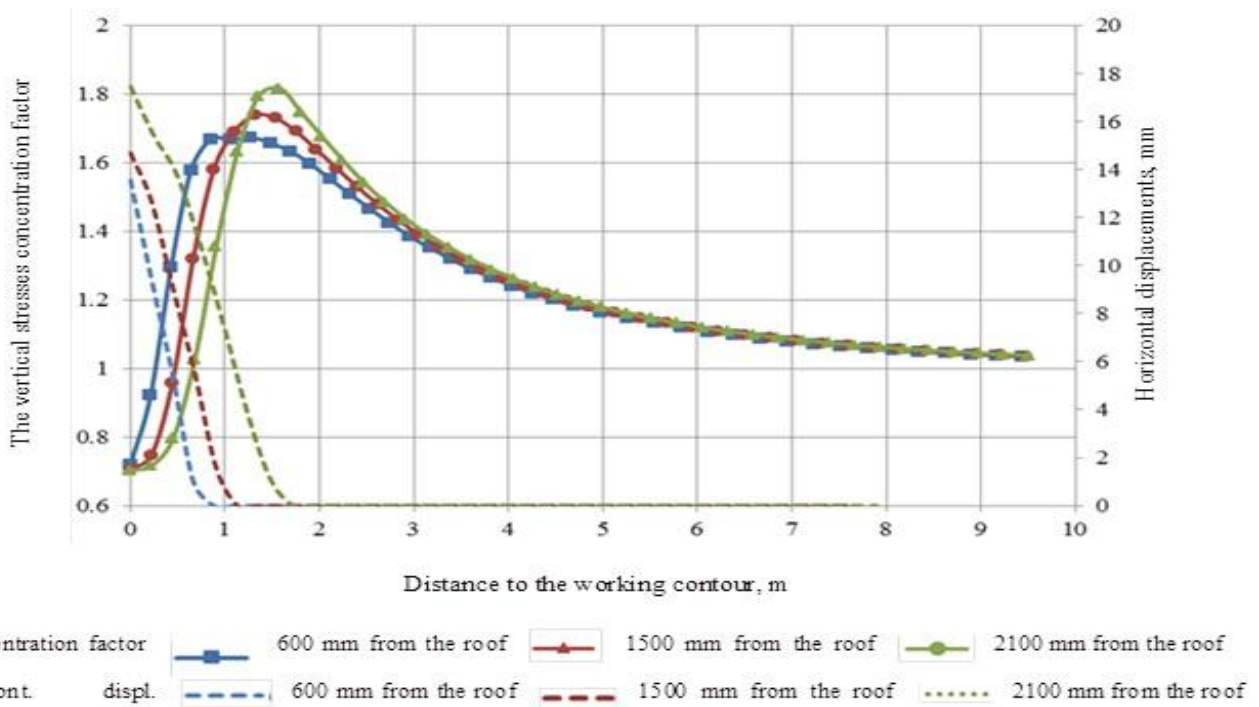


**Figure 4.** Dependence of the vertical stresses concentration and horizontal displacements change on the distance to the single trapezoidal profile working contour

The maximum concentrations of vertical stresses  $k = 1.8$  in the unsupported working wall are observed at the distance of 1.6 m from the working contour. The near-contour zone with the depth of 0-0.7 m is characterized by the lower vertical stresses. The working influence zone is 7 m.

Maximum horizontal displacements of the trapezoidal profile working contour are 17 mm, which is 32% less than the similar index for the rectangular profile working.

The mutual interaction of the two first stage workings driven under the safety overlap at the distance of three spans was explored.

Configuration of the limit state zones along the first stage workings is presented in Figure 5. The limit state zones contour and dimensions are the same as for the single working driving.

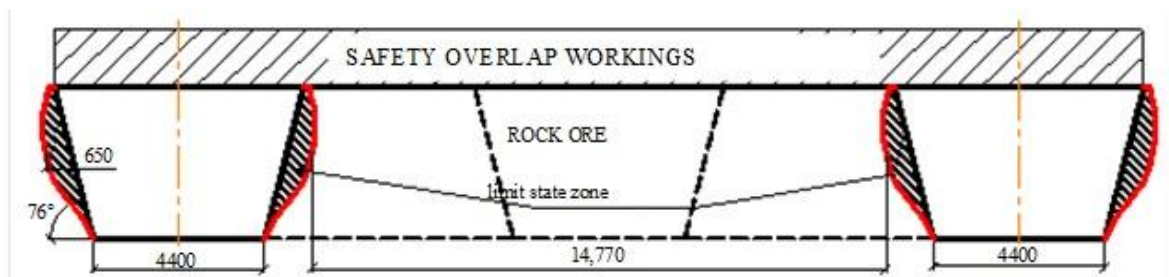


**Figure 5.** The limit state zones formation in the first stage workings under the safety overlap

The dependence of the vertical stresses concentration and horizontal displacements in the rock ore between the first stage workings on the distance to the roof are presented in Figure 6.

It follows from the behavior of the horizontal displacements between the two workings in the rock mass that the workings contour is displaced by the value of 20 mm; the horizontal displacements zone is spread deep into the rock mass at the distance of approximately 2.0 m.

The maximum concentrations of the vertical stresses  $k = 1.85$  are observed at the distance of 1.6 m from the contour. The dividing pillar between the workings is practically entirely located in the higher compression vertical stresses zone at the distance up to 0.7 m from the contour. The vertical stresses decrease and the higher horizontal displacements are the indication of the plastic strains development in the rock ore. The horizontal displacements in the pillar center are equal to zero.

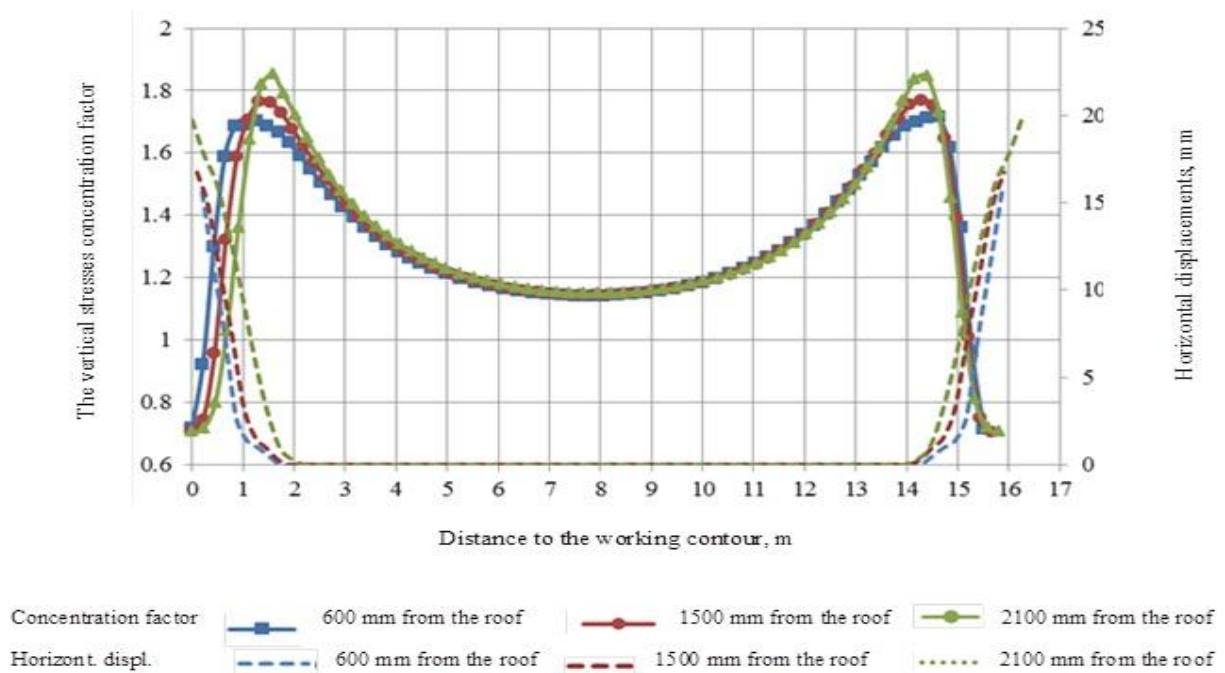


**Figure 6.** Dependence of the vertical stresses concentration and horizontal displacements change on the distance to the contour in the first stage workings walls under the safety overlap

The mutual interaction of the two first stage workings driven along the ore pillar between the first stage filled workings under the safety overlap was explored.

The configuration of the limit state zones along the second stage workings is presented in Figure 7. In this case, the limit state zone depth differs from the similar index for the first stage workings driving by 150 mm, herewith there is an increase of the zone square of 20%.

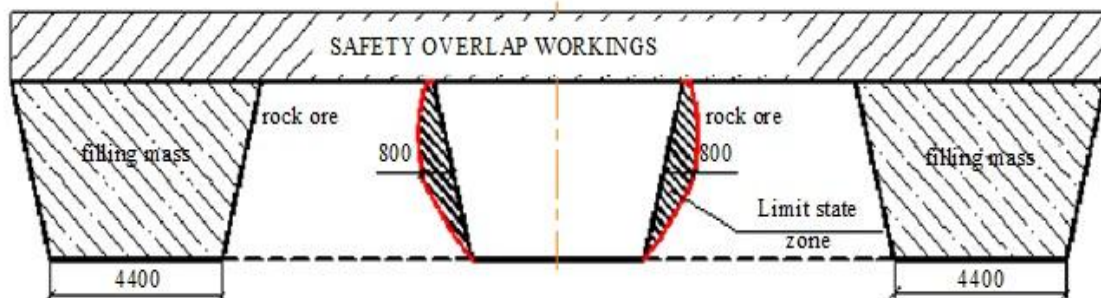


**Figure 7.** The limit state zones formation in the first stage workings walls under the safety overlap

## DISCUSSION

The results of the field studies over the workings stability and numerical experiments indicate that the walls of the rectangular profile working, driven in the friable ores under the safety overlap, lose stability due to the shear surfaces formation in the near-contour rock mass.

For the workings stability improvement it is suggested to change their cross-sectional shape from rectangular to trapezoidal profile.

The first stage trapezoidal profile workings with the long base in the roof should be driven with leaving of the pillar with the width of three spans. After the first stage workings driving, the second stage workings are driven. The third stage workings are driven between two workings filled by the concrete. The present workings configuration meets the present basic criteria: it ensures the safety conditions of the workings maintenance and takes into account the parameters of the selective heading machine used at the presented time at the Yakovlevsky mine.

The configuration and dimensions of the limit state zone around the rectangular profile working in case of the contact with frictional drag coefficient  $F = 0.35-0.45$  are in good agreement with the field studies data. The shear surface is formed at the contact of the rock ore and the safety overlap at the distance of 1.2 m from the working contour and is directed at an angle of  $68^\circ$ .

The horizontal displacements are spread deep into the rock ore at the distance of 3.0 m, the working contour near the roof is displaced by 25 mm. With an increase in the distance to the roof, the working displacements are decreased. The intensive growth of the horizontal displacements is observed at the distance of 1.2 m to the working contour, which corresponds to the limit state domain boundary.

The maximum concentrations of the vertical stresses  $k = 1.62$  are observed at the distance of 2.0 m to the working contour. In the limit state zone – at the distance up to 1.2 m to the working contour –  $k = 0.7-1.0$ . The working influence zone is 8 m.

The limit state domain in the trapezoidal profile working wall is spread deep into the rock ore at the distance of 0.65 m, which is 50% less than the similar index for the rectangular profile working.

The horizontal displacements of the trapezoidal profile working contour are 18 mm, which is 35% less than the similar index for the rectangular profile working.

During the second stage trapezoidal profile workings driving along the ore pillar between the filled first stage workings under the safety overlap, the limit state zone depth differs from the similar index for the first stage workings driving by 150 mm, herewith there is an increase of the zone square of 20%.

## CONCLUSION

For the stopes stability improvement, it is appropriate to move from rectangular to trapezoidal profile.

In this case, it is necessary to justify the trapezoidal profile workings driving procedures. In future, for the mine production capacity improvement and cost reduction of the mined iron ore, it is suggested to consider the switch to the polygonal profile of the stopes with the increased geometric parameters. For this purpose, on the first stage the geomechanical model development and calculation of the ore and rock masses stress-strain behavior are planned.

## REFERENCES

- [1] S.V. Sergeev, A.I. Lyabakh, D.A. Zaitsev, & V.V. Sevryukov, “Inzhenerno-geologicheskoe soprovozhdenie gornyx rabot pri razrabotke rykhlykh rud KMA” [Engineering-Geological Support for Mining Works during the KMA Friable Ores Mining]. Gornyy informatsionno-analiticheskiy byulleten', vol. 11, pp. 41-44, 2011
- [2] “Geologia, hydrogeologia i zheleznie rudy Kurskoy Magnitnoi Anomalii” [Geology, Ground Water Hydrology and Iron Ores of the Kursk Magnetic Anomaly]. Moscow: Nedra, n. d.
- [3] R.E. Dashko, & E.N. Kovaleva, “Kompleksniy monitoring podzemnykh vod na Yakovlevskom mestorogdenii bogatyykh zheleznykh rud i ego rol v povyshenii bezopasnosti vedeniya gornyx rabot v usloviyakh neosushennykh vodonosnykh gorizontov” [Integrated Monitoring of the Ground Waters at the Yakovlevsky Deposit of rich Iron Ores and Its Role in the Mining Safety Improvement under the Conditions of Undrained Water-Bearing Stratum]. Zapiski Gornogo instituta, vol. 190, pp. 78-85, 2011.
- [4] R.E. Dashko, “Inzhenerno-geologicheskaya charakteristika i otsenka bogatyykh zheleznykh rud Yakovlevskogo rudnika” [Engineering-Geological Characteristics and Evaluation of the Rich Iron Ores of the Yakovlevsky Mine]. Zapiski Gornogo instituta, vol. 168, pp. 97-104, 2006.
- [5] V.L. Trushko, A.G. Protosenya, & R.E. Dashko, “Geomekhanicheskie i gidrogeologicheskie problemy osvoyeniya Yakovlevskogo mestorozhdeniya” [Geomechanical and Hydrogeological Problems of the Yakovlevsky Deposit Development]. Zapiski Gornogo instituta, vol. 185, pp. 9-18, 2010.
- [6] R.E. Dashko, & A.V. Volkova, “Issledovanie vozmozhnosti proryvov podzemnykh vod iz nizhnego kamennougolnogo vodonosnogo gorizonta v gornye vyrabotki Yakovlevskogo rudnika” [Study of the Probability of the Ground Waters Breakthrough from the Low Coal Mining Water-Bearing Stratum in the

- Yakovlevsky Mine Working]. Zapiski Gornogo instituta, vol. 168, pp. 142-148, 2006.
- [7] V.L. Trushko, & A.G. Protosenya, "Geomechanical Estimation of Unique Deposits of Soft Iron Ores Under High Pressure Aquifers". Biosciences, Biotechnology Research Asia, vol. 12, no. 3, pp. 2889-2899, 2015.
- [8] A.M. Grigoryev, "Geomekhanicheskiy analiz tselikov i potolochiny pri etazhno-kamernoy sisteme razrabotki Korobkovskogo mestorozhdeniya" [Geomechanical Analysis of Pillars and Foot Pillars in Case of the Pillar-And-Breast System of the Korobkovskoye Deposit]. Gorno-informatsionnyy analiticheskiy byulleten', vol. 7, pp. 205-211, 2008.
- [9] D.M. Kazikaev, & Yu.S. Osipenko, "Razrabotka rudnykh mestorozhdeniy pod vodnymi obyektami" [The Ore Deposits Development under the Water Objects]. Moscow: Nedra, 1989.
- [10] V.P. Zubov, & A.A. Antonov, "Kontseptsia otrabotki Yakovlevskogo zhelezorudnogo mestorozhdeniya na uchastkakh bogatykh zheleznykh rud" [The Concept of the Yakovlevsky Iron Ore Deposit Development at the Rich Iron Ores Areas]. Zapiski Gornogo instituta, vol. 168, pp. 203-210, 2006.
- [11] A.M. Grigoryev, "Geomechanical Maintenance of Flooded Field Mining Problems". In Rock Mechanics: Meeting Society's Challenges and Demands: Proceedings of the 1st Canada-U.S. Rock Mechanics Symposium, Vancouver, Canada, 27-31 May 2007. Vol. 2: Case Histories, pp. 1469-1474, 2007.
- [12] V.N. Kalmykov, & E.Yu. Meshcheryakov, "Geomekhanicheskoye obespechenie gornykh rabot na rudnikakh OAO "Uchalinskiy GOK" [Geomechanical Mining Works Maintenance at the "Uchalinskiy GOK" OJSC Mines]. Ratsionalnoe osvoenie nedr, vol. 1, pp. 62-66, 2010.
- [13] V.S. Litvinenko, R.E. Dashko, V.P. Zubov, A.G. Protosenya, & V.L. Trushko, "Razrabotka i vnedrenie ekologicheskikh chistykh kombinirovannykh tekhnologiy dobychi i kompleksnoy pererabotki rud, obespechivavshikh vvod v ekspluatatsiyu i osvoenie unikalnogo Yakovlenskogo mestorozhdeniya bogatykh zheleznykh rud. Prilozhenie k "Zapiskam Gornogo instituta" [Development and Implementation of Environmentally Friendly Combined Techniques of the Ores Extraction and Integrated Processing, Providing Putting into Service and Development of the Unique Yakovlevsky Deposit of the Rich Iron Ores. Appendix to "Proceedings of the Mining University"]. Saint Petersburg: RIC SPMU(TU), 2007.
- [14] M.D. Morozov, "Prospects for the Introduction of Competitive Technologies Production of Direct Reduced Iron in "Yakovlevsky" Mine". Scientific Reports on Resource Issues TUBAF, vol. 1, pp. 109-112, 2011.
- [15] D.A. Potemkin, "Modelirovanie protsessov sdvizheniya massiva gornykh porod pri niskhodyashchem poryadke otrabotki rudnogo tela Yakovlevskogo mestorozhdeniya" [Modeling of the Rock Mass Displacement in Case of the Yakovlevsky Deposits Ore Body Mining in Descending Order]. Zapiski Gornogo instituta, vol. 168, pp. 137-141, 2007.
- [16] V.L. Trushko, & A.G. Protosenya. "Forecast of Excavation Stability in Friable Iron Ore in Terms of the Yakovlevsky Deposit". Journal of Mining Science, vol. 49, no. 4, pp. 557-566, 2013.
- [17] V.L. Trushko, & A.G. Protosenya, "Geomechanical Models and Prognosis of Stress-strain Behavior of Rock Ore in Development of Unique Deposits of Rich Iron Ores Under Water-bearing Formations". Biosciences, Biotechnology Research Asia, vol. 12, no. 3, pp. 2879-2888, 2015.